A Study on the Structural, Spectral and Nonlinear Optical Properties of R-Phenylalanine-S-Mandelic Acid Single Crystals

K. Sivakumar, M. Senthilkumar & C. Ramachandra Raja*
Department of Physics,
Government Arts College (Autonomous),
Kumbakonam- 612 002, India.

Received Dec. 06, 2017 Accepted Jan. 08, 2018

ABSTRACT *Single crystals of R-Phenylalanine-S-Mandelic acid (RPSM) were grown by slow evaporation solution growth method at 36°C. The lattice parameters of the grown crystal were determined by X-ray diffraction analysis. The vibrations of functional groups in the grown crystal were studied by Fourier transform infrared and Raman Spectral analysis. UV-Vis-NIR transmittance study was carried out to determine the cut-off wavelength and transmission range. The thermal property of the grown crystal was investigated by TG/DTA analysis. The molecular structure of the grown crystal was established by ^{13}C-NMR spectroscopy. Kurtz–Perry test was conducted for the powder form of grown crystal, which showed positive results for second harmonic generation (SHG). Third order nonlinear optical properties were determined by Z-scan technique using He-Ne laser. Closed aperture Z-scan study reveals the positive nonlinearity in the crystal and open aperture Z-scan demonstrates the nonlinear absorption is reverse saturable absorption.*

Keywords: *Crystal growth; XRD; Spectroscopy; NMR; Nonlinear optics; Z-scan.*

1.Introduction

Nonlinear optical organic crystals have been used in harmonic generation, sum and difference frequency generation, electro-optic modulation, optical parametric oscillation, optical bi-stability, etc. [1–3]. These crystals show high optical nonlinearity due to the presence of electron donor and acceptor groups. A number of such crystals with good nonlinear optical properties have been found in recent years [4].

An amino acid based crystal exhibits high nonlinear optical efficiency because of its noncentrosymmetric space group and chiral carbon atom [5-6]. The efficiency can be increased by large delocalized π-electron system with strong donor and acceptor groups [7-8]. Amino acids contain a proton donor carboxyl acid (COO^-) group and the proton acceptor amine group (NH_2^+) with them. Molecular hyperpolarizability β is the basis for a strong second harmonic generation response. Organic crystals usually exhibit high β value and are good candidates for NLO applications [9].

R- Phenylalanine is a amino acid and forms complexes with other organic acids. The structure of RPSM is already reported [10]. However, the nonlinear optical property of RPSM crystal has not been reported so far. Hence in the present work, the nonlinear optical properties of this crystal are studied.

Single crystals of RPSM have been grown by reacting RPA and SMA in 1:1 molar ratio using slow evaporation solution growth method. The grown crystals were characterized by single crystal XRD analysis, Powder XRD analysis, UV-Vis-NIR spectroscopy, FT-IR spectroscopy, FT-Raman spectroscopy, Thermal studies, FT-NMR spectroscopy, Second harmonic generation (SHG) test, Z-scan test and the results are reported.

2 Experimental

2.1 Synthesis

Single crystals of RPSM were grown by reacting RPA and SMA in 1:1 molar ratio by slow evaporation method. 1.521 g of SMA was first dissolved in 100 ml of deionized water. Then 1.651 g of RPA was added to the solution slowly with stirring. The solution was stirred for 4 hours until the solution become completely transparent. This solution was filtered by Whatman filter paper to remove any impurities that may be present and it was closed with a perforated cover. Then the filtered solution was maintained at 36° C using a constant temperature bath with an accuracy of ± 0.1°C. Due to slow evaporation of the solvent the solution become supersaturated. Transparent single crystals of RPSM were grown at the bottom of the beaker in a period of 30 days. The grown RPSM crystal is shown in Fig.1.

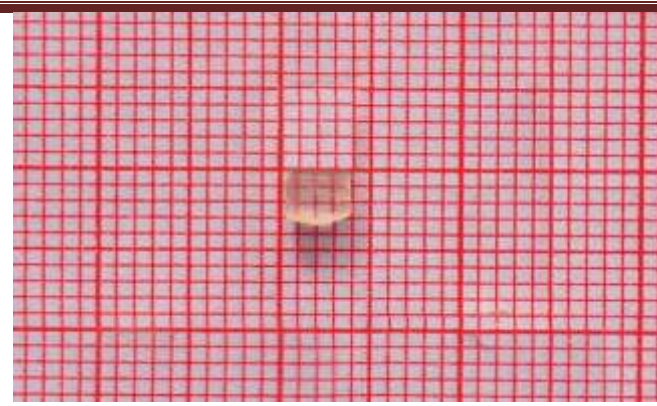

Fig.1 Photograph of RPSM single crystals

2.2 Characterization

Single crystal X-ray diffraction study of the grown crystal was carried out using Bruker AXS kappa Apex2 diffractometer. The powder XRD analysis was carried out using Ultima3 theta-theta gonio X-ray diffractometer. The UV-Vis-NIR spectrum was recorded in the range of 190-1100 nm using lamda 35 double beam spectrometer. Fourier Transform Infrared (FT-IR) spectrum was recorded in the range of 4000–400 cm^{-1} using PERKIN ELMER RX1 spectrometer. The FT-Raman spectrum was recorded in the range of 4000–50 cm^{-1} using BRUKER: RFS 27 spectrometer. Thermal behavior of the grown crystal was studied by TG/DTA analysis using SDT Q600 V20.9 Build 20. The ^{13}C-NMR spectrum of grown RPSM single crystal was recorded using Bruker FT-NMR spectrometer. The SHG efficiency of the crystal was evaluated by the Kurtz and Perry powder technique using a Q-switched, mode locked Nd:YAG laser. In the Z-scan technique, the sample is translated in the Z-direction along the axis of a focused Gaussian beam from the He-Ne laser at 632.8 nm and the far field intensity is measured as a function of the sample position.

3. Result and Discussion

3.1. Single crystal XRD analysis

Transparent crystals of RPSM are subjected to XRD analysis at room temperature to determine the lattice parameters. This shows that the grown crystal belongs to monoclinic crystal system and the measured cell parameters are a= 19.88 ± 0.03 Å, b=5.56 ± 0.009Å, c=17.10 ± 0.03 Å, α = γ= 90, β =123.93 ± 0.02 °, and the cell volume V = 1569 ± 7 $Å^3$**.** These results are in good agreement with the values reported in literature [10].

3.2. Powder XRD analysis

The powder XRD pattern of RPSM crystal is shown in Fig.2. The powdered RPSM sample was scanned over the range 10°–80º at the rate of 1º/ min. Sharp and strong peaks confirmed the good crystallinity of the grown crystal. From the powder X-ray data, the various planes of reflections were indexed using the programme Indx. Using the simulated hkl values and d spacing values, lattice parameters were calculated with the help of programme, Unitcell. The calculated lattice parameters are compared with the lattice parameters obtained from single crystal XRD and presented in Table 1. It shows that the lattice parameters calculated from powder XRD is closely matched with results obtained from single crystal XRD.

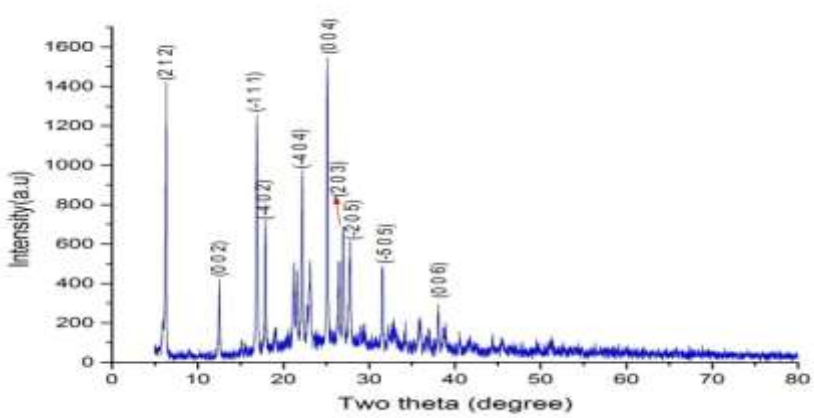

Fig.2. Powder XRD pattern of RPSM crystal

Table 1. Comparison of crystal data of single crystal XRD and powder XRD

XRD Analysis	a (Å)	b (Å)	c (Å)	V (Å)^3
Single crystal XRD	19.88	5.56	17.10	1569
Powder XRD	19.88	5.56	17.08	1567

3.3. UV-Vis-NIR Analysis

The percentage of transmittance vs. wavelength of RPSM crystal is shown in **Fig. 3.** The thickness of the crystal used in this study is 2 mm. The UV- Visible transmission spectrum is very important for optical material because of its wide transmittance window. From this measurement, it is observed that the crystal is transparent in the wavelength range of 351–1100 nm. The UV transparency cut-off wavelength of RPSM single crystal occurs at 351 nm. This suggests that the crystal can be used effectively in converting the Nd:YAG fundamental wavelength, 1064 nm, into its second harmonic, 532 nm and third harmonic, 355 nm.

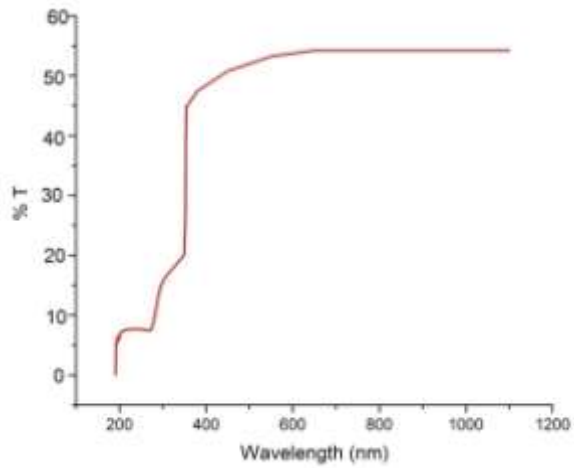

Fig. 3 UV–Vis–NIR spectrum of RPSM crystal

3.4. FT-IR and FT-Raman spectral study of RPSM

The FT-IR and FT-Raman spectra of RPSM single crystal in shown in Fig.4 and Fig.5 respectively. In FT-IR spectrum, the strong band at 3450 cm^{-1} corresponds to OH asymmetric stretching. The peak observed between 2910 cm^{-1} and 3036 cm^{-1}in IR corresponds to $NH_3^+$and CH_2 vibration and the same is observed at 3059 cm^{-1} and 2938 cm^{-1} in FT-Raman spectrum respectively. In the FT-Raman spectrum the peak observed at 1604 cm^{-1} corresponds to C=O stretching and it is observed at 1723 cm^{-1} in FT-IR spectrum. The band present at 1583 cm^{-1} in FT-Raman corresponds to NH_3^+ stretching. The peak at 1454 cm^{-1} in FT-IR and the one at 1439 cm^{-1} in FT-Raman are assigned to COO^- stretching. In FT-Raman spectrum peak observed at 1361 cm^{-1} corresponds to C-N stretching. The peak occurring at 1326 cm^{-1} corresponds to OH in plane bending in FT-Raman. In FT-IR band observed at 1248 cm^{-1} corresponds to C-NH_2 stretching. The sharp peak at 1193 cm^{-1} and 1190 cm^{-1} in FT-IR and FT-Raman respectively corresponds to C-O stretching. The FT-IR and FT-Raman peaks observed at 1063 cm^{-1} and 1029 cm^{-1} corresponds to C-NH_2 stretching. In FT-Raman the peak presents at 1001 cm^{-1} corresponds to C-C-N stretching. The FT-IR and FT-Raman peaks observed at 933 cm^{-1} and 931 cm^{-1} corresponds to C-H out of plane bending. The benzene ring deformation is due to bands at 861 cm^{-1} and 863 cm^{-1} in FT-IR and FT-Raman respectively. The FT-IR and FT-Raman peaks observed at 768 cm^{-1} and 766 cm^{-1} respectively corresponds to CH_2 rocking. The intense sharp band at 727 cm^{-1} and 749 cm^{-1} corresponds to CH_2 rocking vibration. In FT-IR and FT-Raman spectra, the C-C stretching vibration is observed between 480 cm^{-1} and 620 cm^{-1}. All the vibrational bands assigned in IR and Raman spectra have been listed in Table 2. The results are in good agreement with results reported [11-13].

Table 2. FT-IR and FT-Raman assignments of RPSM crystal

FT-IR (cm^{-1})	FT-Raman(cm^{-1})	Assignments
3450	-	O-H asymmetric stretching
2910-3036	3059,2938	NH_3^+ and CH_2 vibration
1723	1604	C=O stretching
-	1583	NH_3^+ stretching
1454	1439	COO^- stretching
-	1361	C-N stretching

-	1326	OH in plane bending
1248	-	C-NH_2 stretching
1193	1190	C-O stretching
1063	1029	C-NH_2 stretching
-	1001	C-C-N stretching
933	931	C-H out of plane bending
861	863	Benzene ring deformation
768	766	CH_2 rocking
727	749	CH_2 rocking vibration
494-616	481-620	C-C stretching vibration

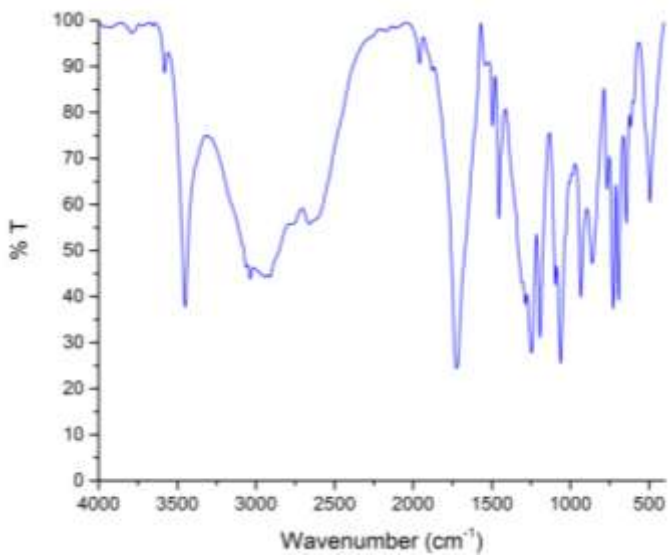

Fig.4. FT-IR spectrum of RPSM crystal

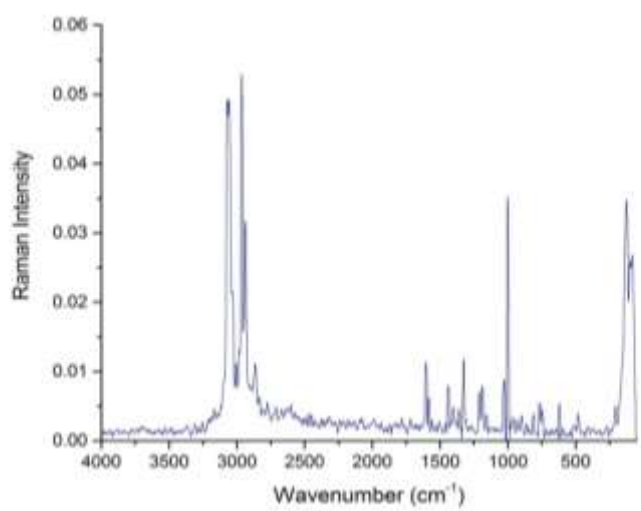

Fig.5.FT-Raman spectrum of RPSM crystal

3.5. Thermal Analysis

The TGA and DTA curve of RPSM crystal is shown in fig.6. A sample of weight 4.614 mg was taken in a crucible. The sample was heated at a rate of 10ºC /min in the nitrogen atmosphere. The TGA curve shows that the crystal is stable up to 161ºC. Then the crystal undergoes complete decomposition in several stages from 161ºC to 610ºC. Differential thermal analysis (DTA) curve shows endothermic peaks at 161ºC, 198ºC and 217ºC. The first endothermic peak may correspond to the melting point of the crystal and the successive peaks are due to the decomposition of the crystal.

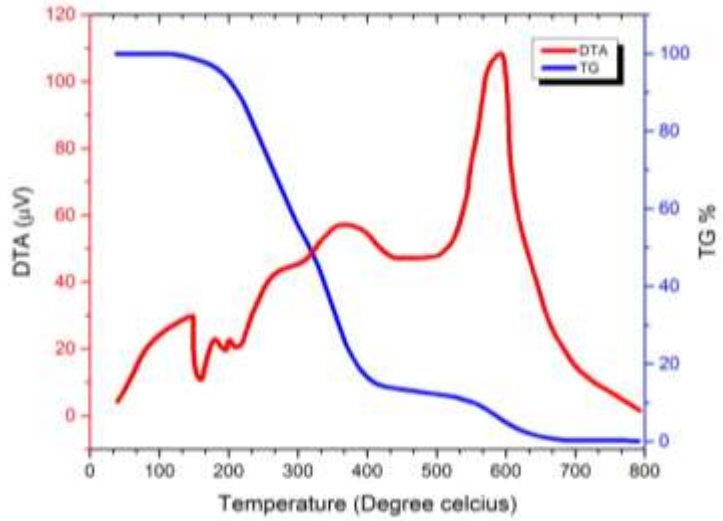

Fig. 6 TG/DTA Curve of RPSM crystal

3.6. NMR Studies

The ^{13}C-NMR spectrum of RPSM crystal is presented in Fig. 8. The chemical shifts are tabulated with assignments in Table 3. The ^{13}C-NMR spectrum of RPSM can be understood with the help of the molecular structure shown in Fig.7 [14].

In ^{13}C-NMR spectrum, the signal observed at 176.74 ppm corresponds to the carbon 1 (COOH group) of R-phenylalanine. The signal observed at 173.36 corresponds to the carbon 1(COOH group) of S-mandelic acid. The signal at 138.41 ppm is due to carbon 2 (group) of S-mandelic acid. The signal at 134.82 ppm is due to carbon 2 (group) of R-phenylalanine. The signals observed at 129.34 ppm, 129.11 ppm and 129.02 ppm are due to carbon 3, 4 and 5 (CH group) of R-phenylalanine. The signals observed at 128.87 ppm, 127.74 ppm and 127.06 ppm are due to carbon 3, 4 and 5 (CH group) of S-mandelic acid. The signal at 73.22 ppm is due to carbon 6 (group) of S-mandelic acid. The signal at 55.60 ppm is due to carbon 6 (group) of R-Phenylalanine. The signal at 36.15 ppm is due to carbon 7 (group) of R-Phenylalanine. The results are in agreement with the reported values [12]. The presence of signals for all the carbon atoms of RPA and SMA confirms the formation of the RPSM molecule.

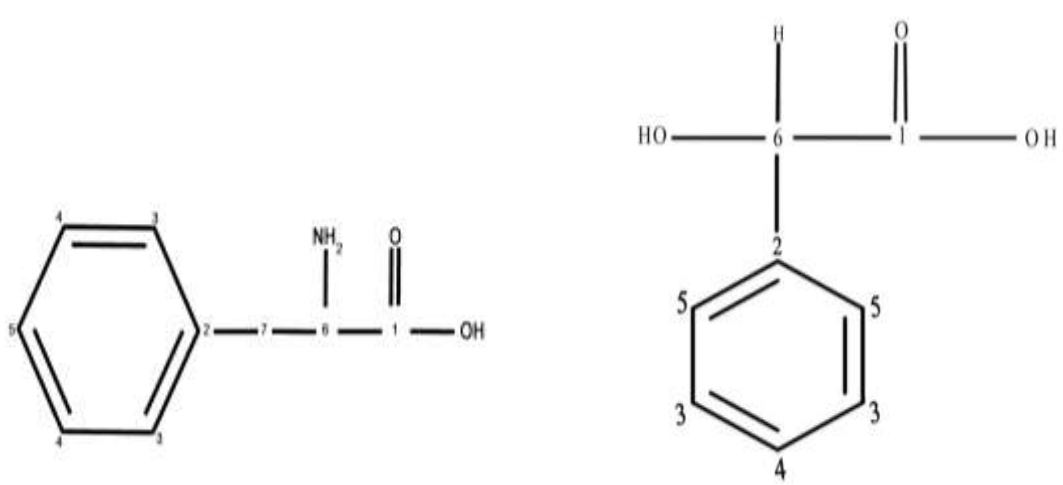

RPA **SMA**

Fig.7 ^{13}C-NMR atomic numbering of RPSM crystal

e ISSN 2348 –1269, Print ISSN 2349-5138
Cosmos Impact Factor 4.236

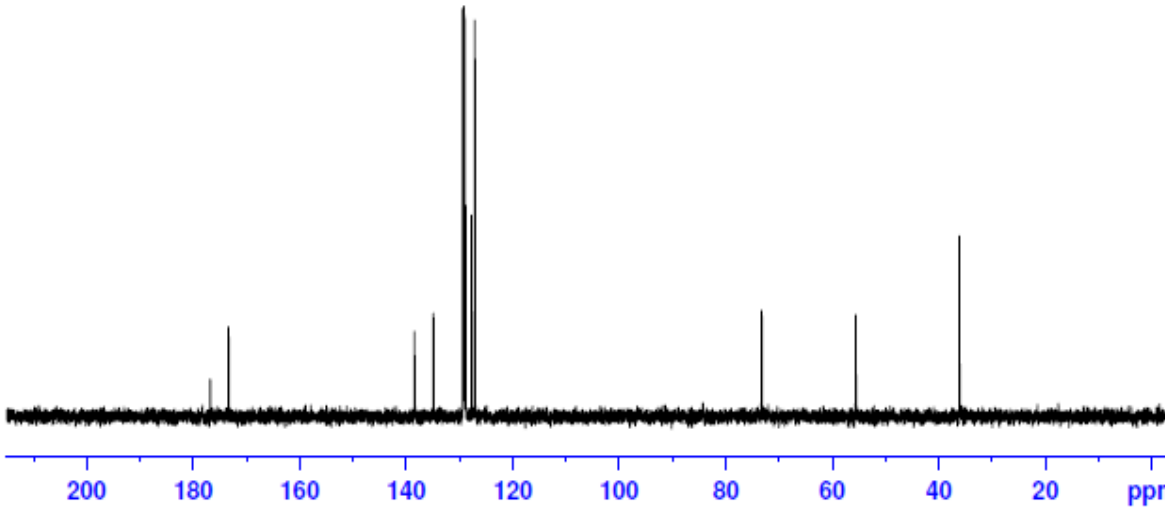

Fig.8 ^{13}C-NMR spectrum of RPSM crystal

Table 3. Chemical shifts in ^{13}C-NMR spectra of RPSM

Chemical shift (ppm)	Group identification
176.74	Carbon 1(COOH group of R-phenylalanine)
173.36	Carbon 1 (COOH group of S-mandelic acid)
138.41	Carbon 2 ( group of S-mandelic Acid)
134.82	Carbon 2 ( group of R-phenylalanine)
129.34	Carbon 3 (CH group of R-phenylalanine)
129.11	Carbon 4 (CH group of R-phenylalanine)
129.02	Carbon 5 (CH group of R-phenylalanine)
128.87	Carbon 3 (CH group of S-mandelic acid)
127.74	Carbon 4 (CH group of S-mandelic acid)
127.06	Carbon 5 (CH group of S-mandelic acid)
73.22	Carbon 6(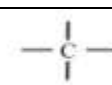 group of S-mandelic acid)
55.60	Carbon 6 ( group of R-phenylalanine)
36.15	Carbon 7 (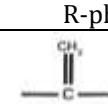 group of R-phenylalanine)

3.7. Second Harmonic Generation Analysis

The Kurtz and Perry method was employed to measure powder SHG efficiency of RPSM single crystals. The grown crystals grind into very fine powder and tightly packed in a micro capillary tube which served as the sample cell. Then it was mounted in the path of Nd:YAG laser with first harmonic output of 1064 nm with the pulse width of 6 ns. The input pulse with energy 0.701 J/pulse is used. Potassium dihydrogen phosphate (KDP) is used as the reference material. The emission of green light of wavelength

532 nm from RPSM crystal confirms the SHG property. The output energy was measured using an energy meter and found to be 6.26 mJ and 8.91 mJ for RPSM and KDP, respectively. The SHG efficiency of RPSM was found to be 0.7 times that of KDP. The second harmonic generation efficiency of a material depends on its molecular structure. The charge transfer across the bonding groups determines the second harmonic generation output. In RPSM single crystal, R-Phenylalanine and S- Mandelic acid are attached through several hydrogen bonds. The SHG efficiency is due to the presence of this hydrogen bond present in the crystal. SHG efficiency of some amino acid and based crystals are presented in Table 4.

Table 4. SHG efficiency of some amino acid based crystals

Crystal	Space group	SHG efficiency	Reference
L-phenylalanine nitric acid	$P2_1$	0.26	15
L-alanine	$P2_1$	0.78	16
L-phenylalanine Benzoic acid	$P2_1$	0.56	17
RPSM	$P2_1$	0.70	**Present work**

3.8. Z-scan Measurement

The third-order nonlinear optical property of RPSM single crystal was studied by Z-scan technique. The nonlinear refractive index (n_2), nonlinear absorption coefficient (β) of RPSM single crystal was evaluated by Z-scan technique. In this method, He-Ne laser of wavelength 632.8nm with beam radius 2 mm was used to scan the sample. Nonlinear refractive index (n_2) was calculated by the relation,

$$n_2 = \frac{\Delta\varphi}{K\ I_0\ L_{eff}}$$

Where $K = 2\pi / \lambda$, I_0 is the intensity of the laser beam at the focus (Z=0), L_{eff} is effective thickness of the sample which was estimated by the relation,

$$L_{eff} = [\ 1- \exp(-\alpha L)\ ] \ / \ \alpha$$

Here α-represents linear absorption coefficient and L is thickness of sample (1mm). Closed aperture Z-scan curve was shown in Fig.9. In closed curve, valley followed by peak reveals the positive nonlinear refractive index (n_2) of material. This suggests that crystal having self-focusing nature.

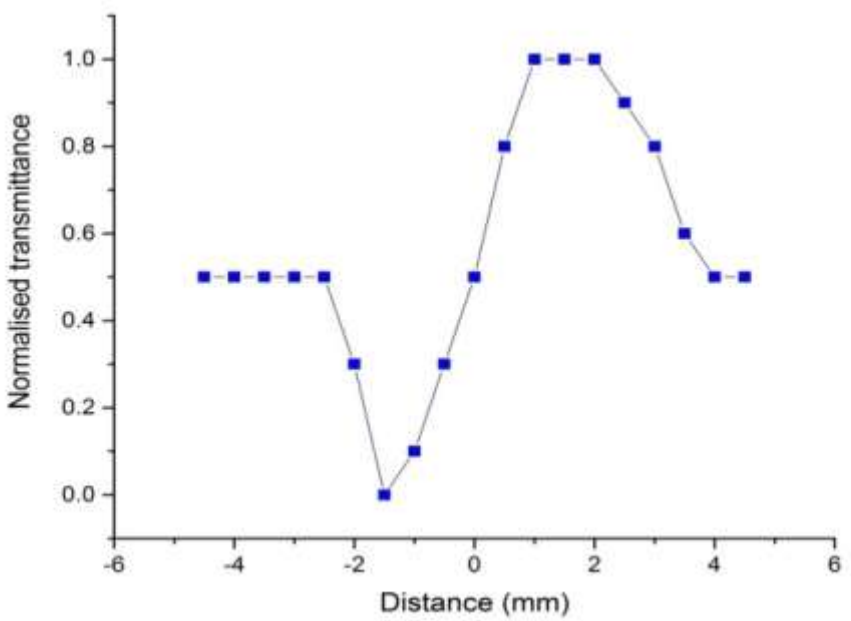

Fig.9 Closed aperture Z-scan pattern of RPSM crystal

From the open aperture Z-scan data, the nonlinear absorption coefficient (β) is estimated using the expression,

$$\beta = \frac{2\sqrt{2}\,\Delta T}{I_0\ Leff}$$

Where $\Delta T = 1-T_v$. (T_v - valley value at the open aperture Z-scan curve). Fig.10 represents the open aperture Z-scan curve. In the figure, minimum transmission occurs near the focus. This is due to reverse saturable absorption of the material [18].

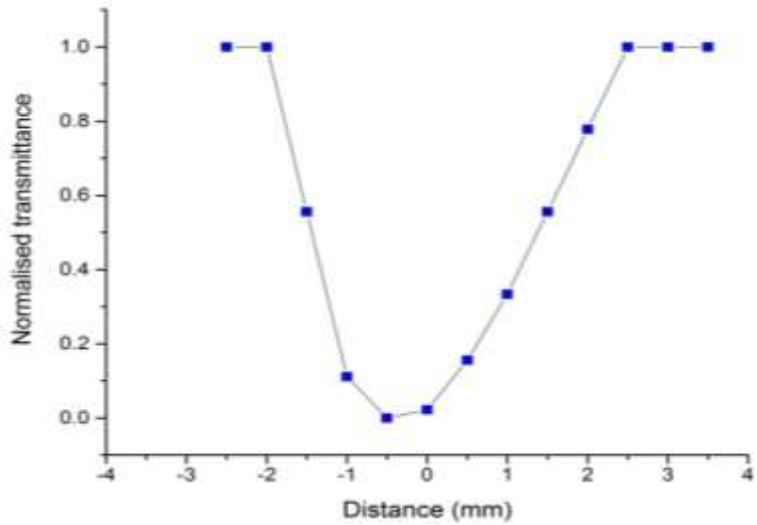

Fig.10 Open aperture Z-scan pattern of RPSM crystal

The real and imaginary parts of the third order nonlinear optical susceptibility $\chi^{(3)}$ are defined as

$$\text{Re}\,\chi^{(3)}\ \text{esu} = 10^{-4}\,\varepsilon_0\,c^2\,n_0^2\,n_2\,/\,\pi \quad (\text{cm}\,/\,\text{V})^2$$

$$\text{Im}\chi^{(3)}\ \text{esu} = 10^{-2}\,\varepsilon_0\,c^2\,n_0^2\,\lambda\,\beta\,/4\pi^2 \quad (\text{cm}\,/\,\text{V})^2$$

Where ε_0 is the vacuum permittivity, n_0 is the linear refractive index of the sample and c is the velocity of light in vacuum. The absolute value of χ (3) is calculated from

$$\chi^3 = \sqrt{[\,\text{Re}\,(\chi^3)\,]^2 + [\,\text{Im}\,(\chi^3)]^2}$$

The nonlinear parameters such as nonlinear refractive index (n_2), nonlinear absorption coefficient (β) and nonlinear susceptibility (χ^3) have been evaluated and tabulated in Table 5.

Table 5. Measurement details and the results of the Z- scan technique

Laser beam wavelength (λ)	632.8 nm
Lens focal length (f)	22.5 cm
Optical path distance (Z)	115 cm
Spot-size diameter in front of the aperture (ω_a)	1 cm
Aperture radius (r_a)	2 mm
Incident intensity at the focus (Z=0)	3.13 MW/Cm^2
Nonlinear refractive index (n_2)	9.559 x 10^{-12} (cm/V)^2
Nonlinear absorption coefficient (β)	0.267 x 10^{-4} (cm/V)^2
Real part of the third-order susceptibility [Re (χ3)]	1.29 x 10^{-8} esu
Imaginary part of the third-order susceptibility [Im (χ3)]	1.82 x 10^{-7} esu
Third-order nonlinear optical susceptibility (χ3)	1.28 x 10^{-7} esu

Conclusion

Single crystals of RPSM have been successfully grown from an aqueous solution using slow evaporation technique. Single crystal and Powder X-ray diffraction studies confirm the monoclinic crystal structure. UV-Vis-NIR spectrum reveals the cut-off wavelength at 351 nm. The vibrations of functional groups were identified by FTIR and FT-Raman spectra. Thermal studies reveal the crystal is stable up to 161°C. The molecular structure of the grown crystal was established by ^{13}C-NMR spectroscopy. The second harmonic generation efficiency of RPSM crystals was confirmed by green colour emission. Third order nonlinear optical properties are calculated using Z-scan technique.

Acknowledgements

Author C.R acknowledges Council of Scientific and Industrial Research (CSIR), New Delhi for financial aid (scheme no: 03(1301)/13/EMR II). The authors are very grateful to Dr. P.K. Das, Indian Institute of Science, Bangalore (IISc) for measurement of SHG efficiency, SAIF, Indian Institute of technology (IIT), Chennai for single crystal XRD and FT-Raman analysis, National institute of technology (NIT), Trichy

for powder XRD and Z-scan studies, Sastra University, Thanjavur for FT- NMR studies and St. Joseph's College, Trichy for FT-IR.

References

1. D. S. Chemla, J. Zyss (Eds.), Nonlinear Optical Properties of Organic Molecules and Crystals, Academic Press, New York, 1987.
2. J. F. Nicoud, Molecular and crystal engineering for organic Nonlinear optical materials, Mol. Cryst. Liq. Cryst. 156 (1988) 257-268.
3. D. F.Eaton, Nonlinear optical materials, Science 253 (1991) 281-287.
4. J. Zyss, Molecular Nonlinear Optics Materials, Physics, and Devices, Academic press / Harcourt Brace and Jovanovich, New York, 1994.
5. M. Kitazawa, R. Higuchi, and M. Takahashi, "Ultraviolet generation at 266 nm in a novel organic nonlinear optical crystal: lpyrrolidone- 2-carboxylic acid," Appl. Phys. Lett. 64 (1994) 2477-2479.
6. L. Misoguti, A. T. Varela, F. D. Nunes et al., "Optical properties of L-alanine organic crystals", Opt. Mater. 6 (1996) 147-152.
7. J. Zyss, "Hyperpolarizabilities of substituted conjugated molecules. III. Study of a family of donor-acceptor disubstituted phenyl-polyenes", J. Chem. Phys. 71 (1979) 909-917.
8. B. F. Levine, C.G. Bethea, R. D.Thermond, R. T. Lynch, and J. L. Berstein, "An organic crystal with an exceptionally large optical second-harmonic coefficient: 2-methyl-4-nitroaniline," J. Appl. Phys. 50 (1979) 2523-2527.
9. P. S. Patil, S. M. Dharmaprakash, K. Ramakrishna, H. Fun, R. S. Kumar, and D. N. Rao, "Second harmonic generation and crystal growth of new chalcone derivatives," J. Crys. Growth 303 (2007) 520-524.
10. K.OKAMURA, K. A0E, H. HIRAMATSU, N. NISHIMURA,T. SATO and K. HASHIM0T0, Crystal Structures of Diastereomeric 1:1 Complexes of (*R*)- and (*S*)-Phenylalanine (*S*)-Mandelic Acid, Anal. sci. 13 (1997) 315-317.
11. M. Prakash, D. Geetha, M. Lydia Caroline, Growth and characterization of Nonlinear Optics (NLO) active L-phenylalanine fumaric acid (LPFA) single crystal, Mater. Manuf. Processes 27 (2012) 519-522.
12. M. Babij, A. Mondry, Synthesis, structure and spectroscopic studies of europium complex with S (+)- mandelic acid, J. rare earth. 29 (2011) 1188-1191.
13. George Socrates, Infrared and Raman Characteristic Group Frequencies, John Wiley
14. & Sons Publishers, 3rd edn., England, 2001.
15. Spectral database for organic compounds (SDBS), http://sdbs.db.aist.go.jp/sdbs/cgi-bin/direct_frame_top.cgi.
16. M. Lydia Caroline, S. Vasudevan, Growth and characterization of L-phenylalanine nitric acid, a new organic nonlinear optical material, Mater. Lett. 63 (2009) 41-44.
17. P. Vasudevan, S. Sankar and D. Jayaraman, Synthesis and Characterization of L-Methioninium Nitrate Single Crystal for Nonlinear Optical Applications, IJCRGG 5 (2013) 2018-2026.
18. M. Prakash, D. Geetha, M. Lydia Caroline, Synthesis, structural, optical, thermal and dielectric studies on new organic nonlinear optical crystal by solution growth technique, Spectrochim. Acta A 107 (2013) 16-23.
19. T. C. Sabari Girisun, S. Dhanuskodi, Linear and nonlinear optical properties of tristhioureazinc sulphate single crystals, J. Cryst. Res. Technol. 44 (2009) 1297-1302.